Hydrological Processes

WILEY

RESEARCH ARTICLE OPEN ACCESS

Variability in Hydrologic Response to Wildfire Between Snow Zones in Forested Headwaters

Q. M. Miller[1] | D. M. Barnard[2] | M. G. Sears[1] | J. C. Hammond[3] | S. K. Kampf[1]

[1]Department of Ecosystem Science and Sustainability, Colorado State University, Fort Collins, Colorado, USA | [2]Water Management and Systems Research Unit, USDA Agricultural Research Service, Fort Collins, Colorado, USA | [3]U.S. Geological Survey, Maryland-Delaware-D.C. Water Science Center, Catonsville, Maryland, USA

Correspondence: Q. M. Miller (millerquinnm@gmail.com) | S. K. Kampf (stephanie.kampf@colostate.edu)

Received: 20 November 2024 | **Revised:** 24 April 2025 | **Accepted:** 25 April 2025

Funding: This work was supported by National Science Foundation.

Keywords: mountain hydrology | rainfall runoff | seasonal snow zone | snow persistence | wildfire

ABSTRACT

Rising temperatures and shifting fire regimes in the western United States are pushing fires upslope into areas of deep winter snowpack, where we have little knowledge of the likely hydrologic impacts of wildfire. We quantified differences in the timing and magnitude of stormflow responses to summer rainstorms among six catchments of varying levels of burn severity and seasonal snowpack cover for years 1–3 after the 2020 Cameron Peak fire. Our objectives were to (1) examine whether responsiveness, magnitude, and timing of stormflow responses to rainfall vary between burned and unburned catchments and between snow zones, and (2) identify the factors that affect these responses. We evaluated whether differences in storm hydrograph peak flow, total flow, stage rise, and lag to peak time differed by snow zone and burn category using generalised linear models. Additional predictors in these models are the maximum 60-min rainfall intensity for each storm, the cumulative potential water deficit prior to the storm, and the year post-fire. These models showed that the high snow zone (HSZ) has higher total stormflow than the low snow zone (LSZ), likely due to the higher soil moisture content in that area. In both snow zones, the biggest driver of the magnitude of the stormflow response was MI_{60}. Burn category did not have a clear impact on stormflow response in the HSZ, but it did impact stage rise at the severely burned catchment in the LSZ. This was the only site that had widespread overland flow post-fire. These results demonstrate that the stormflow responses to fire vary between snow zones, indicating a need to account for elevation and snow persistence in post-fire risk assessments.

1 | Introduction

Much of the contiguous western U.S. ("the West") relies on streamflow from mountainous forested catchments for their freshwater supply (Brown et al. 2008; Viviroli et al. 2007). These regions have experienced increases in the size, duration, and severity of wildfire in recent decades (Calder et al. 2015; Westerling 2016). Though fire is a natural process vital to maintaining ecosystem health in western forests, the changing wildfire regime is likely to impact water quality and availability to western communities (Barnard et al. 2023; Rocca et al. 2014). As population density increases along the wildland –urban interface in the West, it is critical to understand how fire impacts streamflow generation in forested headwaters (Hallema et al. 2018).

Though many studies have documented how fire alters hydrologic processes at the local or regional scale, hydrologic responses to wildfire vary across regions differentiated by climate, topography, soil type, and vegetation (Hallema et al. 2017). Vegetation loss leads to more net precipitation reaching the ground (Cawson et al. 2013; Hallema et al. 2017; Kunze and Stednick 2006).

Surface soil sealing, loss of soil organic matter, increases in soil-water repellency, and other fire-induced changes often lead to reduced infiltration and decreased hydraulic conductivity (Ebel and Moody 2013). This can lead to greater overland flow during rain storms, causing increased post-fire stormflow and greater risk of flooding (Hallema et al. 2017; Moody et al. 2013). Post-fire stormflow responses to rain often decline after vegetation regrows and restores infiltration capacity to the soil (Wilson et al. 2018).

This study focuses on post-fire hydrologic responses in northern Colorado, a region where most post-fire assessments have been conducted for montane forests containing primarily ponderosa pine (*Pinus ponderosa*) at around 1600–2600 m. Though this region historically experienced frequent, low-severity fires, high-severity fires have become more common in the past few decades (Fornwalt et al. 2016; Hallema et al. 2017; Moody et al. 2013). The ponderosa pine zone has mean annual precipitation ranging from 400 to 600 mm and a semi-arid climate. Ponderosa pine is found mainly in the intermittent snow zone: locations where snow frequently falls during the winters but does not last throughout the winter (Richer et al. 2013). Streams in this zone have seasonal patterns, with a small increase during snowmelt runoff and very little flow the rest of the year (Harrison et al. 2021). After fire, the stormflow generation during high-intensity summer rain storms increases due to reduced infiltration capacity and overland flow. This can lead to soil erosion, floods, and debris flows (de Dios Benavis-Solorio and MacDonald 2005; Hallema et al. 2017).

Much less is known about post-fire hazards and their potential triggers in high elevation (> 2600 m) parts of Colorado that experience deep accumulation of winter snow. Subalpine forests in the Front Range have historically experienced infrequent high severity fires on time scales ranging from one to multiple centuries (Rocca et al. 2014), so the responses of streams to fire in these zones have not been documented. The hydrology in these higher elevations is quite different from the intermittent snow zone. Precipitation increases rapidly with elevation above 2600 m, reaching as high as 1500 mm mean annual precipitation (Richer et al. 2013). This area is called the seasonal snow zone because it accumulates snow that persists throughout the winter. Snowmelt during the late spring and early summer leads to a large snowmelt runoff pulse in streams, and streams in this zone export over 50% of precipitation, compared to < 20% in the intermittent snow zone.

Climate change projections indicate that within 50 years high elevation, high-severity fires could recur on the scale of decades, rather than centuries (Westerling et al. 2011), making it important to know what types of post-fire hydrologic changes to expect. The advance of fires to higher elevation is already underway, with fire activity increasing disproportionately in high-elevation mountain regions. Fires have advanced upslope ~500 m in the Front Range (Alizadeh et al. 2021), and the proportion of area burned in the late snow zone has increased (Kampf et al. 2022).

To understand the broader implications of the changing fire regime in this region and how it might impact stormflow, this study examines the hydrologic response to the 2020 Cameron Peak fire. The fire was the largest in Colorado history and burned across a broad elevation gradient (1646–3589 m), including both intermittent and seasonal snow zones. This makes it an ideal case study for comparing how post-fire streamflow generation varies with seasonal snow cover. To that end, this research uses observations from streams located at different elevations and with varying burn severity to quantify the magnitude and timing of stormflow pulses following summer rain storms for the 3 years immediately following the fire. The objectives of this work are to (1) examine whether responsiveness, magnitude, and timing of stormflow to rainfall vary between burned and unburned catchments and between snow zones, and (2) identify the factors that affect these responses.

2 | Methods

2.1 | Site Description

The Front Range, spanning from central Colorado to southern Wyoming, is the meeting point of the easternmost Rocky Mountains and the Great Plains. Along the northern Colorado, portion of the Front Range, the Cache la Poudre River Basin covers 4824 km^2. Today, the basin supplies water to the cities of Fort Collins and Greeley, as well as numerous agricultural areas. It ranges from 1406 to 4125 m elevation, and vegetation and climate vary substantially along this gradient (Addington et al. 2018; Richer et al. 2013). At its highest elevations (> 3000 m), the basin is characterised by dense subalpine spruce-fir forest (*Abies lasiocarpa*, *Picea engelmannii*). At mid-high elevations (~2500–3000 m) the landscape transitions to a mixed-conifer forest, composed mainly of lodgepole pine, Douglas fir (*Pseudotsuga menziesii*), and quaking aspen (*Populus tremuloides*). At its lower elevations (< 2500 m), the forest gives way to scattered ponderosa pine stands (*Pinus ponderosa*) and prairie grasses and shrubs. The basin's mean annual precipitation ranges from around 1000 mm at the high elevation headwaters to 330 mm in the grasslands (Richer et al. 2013). Soil moisture content follows this pattern of precipitation, remaining high in the headwaters where lower temperatures lead to less evaporation (Addington et al. 2018).

Previous research in this area has identified three distinct patterns of snow cover across this elevation gradient. The high elevation seasonal snow zone was divided into two separate components. The persistent snow zone above ~3000 m has deep and lasting snow throughout the winter, and snow typically does not melt until May. The transitional snow zone extends from the lower limit of the persistent snow zone to ~2600 m and consistently has winter snow, but snow melts in April, earlier than in the persistent snow zone. The intermittent snow zone characterises the lower elevations where winter snow cover is typically discontinuous (Moore et al. 2015; Richer et al. 2013). Peak streamflow is snowmelt-dominated in the persistent and transitional snow zones, shifting to rainfall-dominated in the intermittent snow zone (Kampf and Lefsky 2016). During the summer months, particularly July and August, precipitation in this region comes in the form of convective storms that have high spatial and temporal variability and may have high rainfall intensity (Ebel et al. 2012; Smith et al. 2014).

By the summer of 2020, bark beetle attacks and drought had left a large portion of the high elevation forest in the Cache la Poudre basin either dead or water stressed (BAER 2020). The Cameron Peak fire began in these headwaters on August 13, 2020, and spread rapidly. By the time it was contained in December, it had burned 844 km^2, making it the largest fire in Colorado history (BAER 2020). Post-fire soil burn severity mapping indicates that 20% of the area within the fire perimeter was unburned; 44% was burned at low severity; 30% was moderately burned, and 6% was burned at high severity (Figure 1).

For this study, six catchments were selected: five in the Cache la Poudre basin and one in the adjacent Big Thompson basin to span gradients in snow persistence and burn severity. The catchments included one unburned (UB), one moderately burned (MB), and one severely burned (SB) in each of two snow zones, which we call the high snow zone (HSZ) and the low snow zone (LSZ). The HSZ catchments are in the persistent snow zone, and the LSZ catchments are within the transitional and intermittent snow zones (Figure 1). For the burned study catchments, the Monitoring Trends in Burn Severity (MTBS) map was used to determine what percentage of the catchment fell into each burn severity category. The moderately burned sites in each snow zone were burned at moderate and high severity over 24%–31% of their area, whereas the severely burned sites had 54%–78% of area burned at moderate and high severity. Exact matches of burn severity between snow zones were not possible given the heterogeneity in burn patterns. The catchments range in size from 1 to 4 km^2 and have slopes ranging from 8° to 33° (Table 1).

2.2 | Data Collection and Processing

The study catchments were instrumented to continuously monitor rain and stream stage for 2021–2023, years 1–3 post-fire. Rain data was derived from both the National Severe Storms Laboratory Multi-Radar/Multi-Sensor System (MRMS); there were tipping bucket rain gauges at four study catchments, but two of the catchments did not have rain gauges within their drainage areas. For this reason, we used MRMS to ensure consistency in the rain data source between catchments. The MRMS dataset is a radar-derived product that integrates multisensor data, with a spatial resolution of 1 km^2 and a temporal resolution of 2 min (Zhang et al. 2016). Several studies have evaluated MRMS against tipping bucket data and found acceptable agreement (Bayabil et al. 2019; Moazami and Najafi 2021; Rivera-Giboyeaux and Weinbeck 2024).

Stream stage was continuously monitored at the catchment outlets using either capacitance rods (TruTrack WT-HR 1000 mm, Auckland, NZ) or unvented pressure transducers (In Situ Rugged TROLL, Fort Collins, CO, USA; HOBO Water Level Data Logger—U2, Onset Computer Corporation, Bourne, MA, USA). Sites monitored with pressure transducers also had In Situ Rugged BaroTROLL sensors installed to record and correct for atmospheric pressure. For UB HSZ we used discharge data from the USGS (gage number 06614800; U.S. Geological Survey 2024a, 2024b), accessed using the "dataRetrieval" package (de Cicco et al. 2024) in R version 2.7.18 (R Core Team 2024). Stream stage at all sites was recorded every 15 min except at SB LSZ, which recorded at 5-min intervals because the high burn severity in the vicinity of the gage indicated that a dynamic stream response to large rain storms was likely.

Due to quality issues for data recorded at MB LSZ, we used stage data provided by Larimer County, Colorado, USA (Miller et al. 2025). The county data in 2023 were anomalously high compared to previous years, and such high flows were not evident in any other catchment, leading us to conclude that these values were incorrect. For this site, we therefore used only data from 2021 and 2022. The county gage at MB LSZ reported in hourly time steps.

For each site, we conducted quality reviews of the stage data to identify and remove any time periods where the sensors were not working properly. Indications of sensor error are time periods when the stage measurement diverges from the seasonal hydrograph signal, such as large high or low spikes that are not in the shape of hydrographs. Next, we offset-adjusted the stage measurements for time periods when the sensor was downloaded or when the stream channel bed changed. During site visits, conducted approximately monthly during April through September, stream stage was noted from staff plates affixed to the PVC pipes housing the sensors. The staff plate was used as the reference stage; starting at the beginning of each flow season in April, we offset-adjusted the sensor stage to match the field staff plate stage. Then we plotted the stage time series along with the subsequent field stage measurements. If a subsequent field stage measurement did not match the sensor stage, we looked back through the stage record to identify when an offset happened. Offsets were common during sensor download, and these were adjusted to bring the sensor stage back in line with the field stage. At SB and MB LSZ and SB HSZ, changes in the channel cross section during rain storms also affected stage records. To account for these changes, during each field visit, the change in bed position relative to the gage bottom was also recorded. Wherever we identified an offset between field and sensor stage that did not align with data download, we looked back to the previous storm hydrographs to identify when the offset happened. This process is unfortunately somewhat subjective, but the signals we found were typically changes in the baseflow stage from before to after the rain storm. We reviewed the field measurements of bed elevation change and compared those to the baseflow stage changes to ensure that they were consistent. Then we offset-adjusted the stage so that the sensor values matched the field measurements. We did not conduct cross section surveys during each site visit, as it was more than we could accomplish in the time available, but in hindsight, this would have been beneficial to have added for more detailed information about channel changes.

To develop rating curves relating stream stage to discharge, streamflow was measured during each site visit using either salt-dilution gauging or manually with a velocity metre along a channel rcross-section. These stage data were used to develop stage-discharge rating curves (JMP Pro Version 15.2.1) and calculate continuous discharge ($L\,s^{-1}$) at each site (Figure S1). SB and MB LSZ and SB HSZ experienced large movements of sediment during the study period that reconfigured the active channel morphology. Because of this, we had to develop multiple rating curves for those sites. Given the channel morphology changes and other sources of uncertainty in stage-discharge

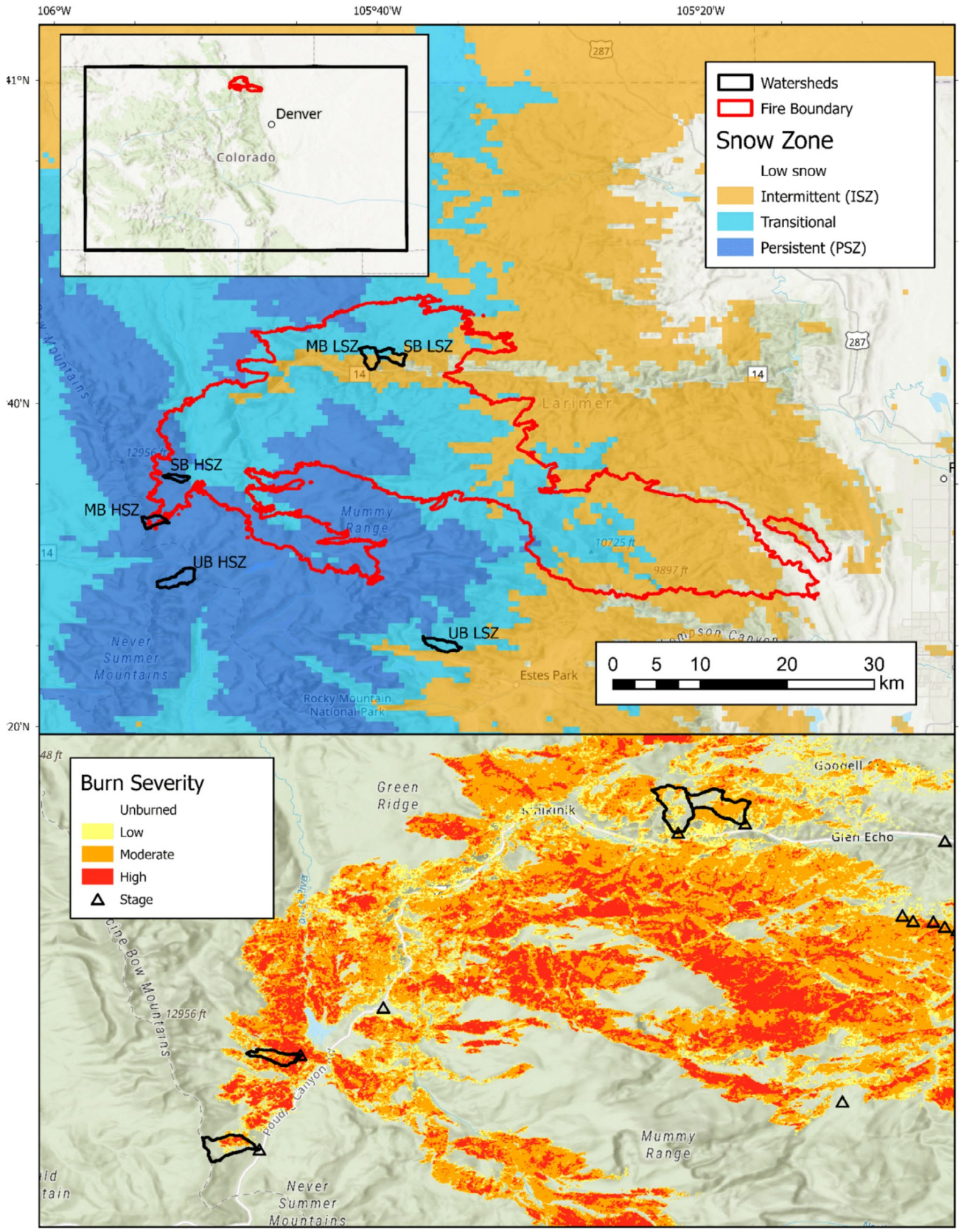

FIGURE 1 | Map of the study area. The top map shows the outline of the Cameron Peak fire over a map of snow persistence, delineated into three zones of coverage [intermittent snow zone (ISZ), transitional snow zone (TSZ), and persistent snow zone (PSZ)] (Hammond 2020; Moore et al. 2015), and the six study catchments (UB- unburned; MB- moderately burned; SB- severely burned). The bottom map shows a soil burn severity map of the Cameron Peak fire (MTBS Data Access 2017) along with the study catchments and stream gages. Basemap *Source:* Esri World Street Map.

TABLE 1 | Study catchment characteristics. All characteristics, except for Snow Persistence and Percent Burned, were determined in ESRI ArcGIS Pro using a U.S. Geological Survey 1 m LiDAR DEM. Snow persistence, which refers to the percent of time between January 1 and July 3 that the ground is snow-covered, was obtained for the years 2001–2020 from the USGS (Hammond 2020). Percent Burned, and percent in each burn severity category were obtained from the Monitoring Trends in Burn Severity map.

Snow Zone	Low snow zone (LSZ)			High snow zone (HSZ)		
Burn Category	Unburned (UB)	Moderate (MB)	Severe (SB)	Unburned (UB)	Moderate (MB)	Severe (SB)
Catchment Name	Bighorn Creek	Washout Gulch	Dry Creek	Michigan River	Montgomery Creek	Blue Lake tributary 4
Mean Slope (^{0})	19	33	18	22	8	13
Aspect	SE	E/SE	E/SE	N/NE	E/SE	E/NE
Area (km^2)	3.0	2.7	2.5	3.9	1.9	1.0
Mean Elevation (m)	2988	2455	2753	3367	3070	3065
Mean Snow Persistence	61.2	54.5	52.5	89.8	87.1	83.3
Percent Burned	0	55	70	0	44	90
Low	0	31	16	0	12	12
Moderate	0	23	52	0	19	38
High	0	1	2	0	12	39
Total Mod-High	0	24	54	0	31	78

rating curves, we estimated discharge uncertainty for each site (Figure S1). The discharge values were normalised by drainage area to facilitate comparisons between catchments and are given in millimetres.

2.3 | Stormflow Responses to Rainfall

The study catchments experience both snowmelt and rainfall runoff. Our focus was on rainfall runoff, so we restricted the study time period to June–September, the months that do not have snow storms in this region. At the LSZ catchments, the snowmelt runoff hydrographs lasted only until April, so June–September reliably had only rainfall runoff. The HSZ catchments could have snowmelt runoff signals continuing into June; we identified these by looking for diurnal changes in stage that are indicative of snowmelt.

For the time periods identified at each catchment, rain storms were defined from precipitation data based on a separation of at least 6 h with less than 1 mm of rain. For each storm, we calculated the total depth of precipitation (P; mm), duration of rain storm (T_{storm}; h), and the maximum intensities (mm h^{-1}) over 30- and 60-min intervals (MI_{30} and MI_{60}). Once the storms were identified for each catchment, the streamflow response to each rain storm was quantified. The stormflow response referred to in the results is the storm hydrograph signal alone, which does not include the gradually varying baseflow. To separate the stormflow (quickflow) and baseflow, we used a digital baseflow separation filter from the 'grwat' package in *R* (Samsonov 2023). This method of recursive digital filtering that applies a one-parameter signal processing filter (Lyne and Hollick 1979). We used 0.99 for the filter parameter value with three passes over the data. This parameter value was identified by iteratively changing the filter parameter until we found the best separation of storm hydrographs from gradually varying baseflow. The parameter value is higher than the 0.925 value used by Nathan and McMahon (1990), as that number was developed for daily flow data and did not adequately separate the baseflow from the stormflow for our shorter time-step data.

To determine whether each rain storm had a stormflow response, we evaluated each rain storm for an accompanying stormflow hydrograph rise. The search window for a hydrograph response was the period between the start of the rain storm and 15 h after. This time window was determined after a visual assessment of all the rain storms and storm hydrographs. Rain storms with an associated hydrograph rise smaller than background noise were eliminated from further consideration. Background noise for each site was determined monthly by filtering out the 24 h of stormflow data following each rain storm and anomalous data spikes, and then taking the maximum stormflow value of the remaining data to represent background noise.

Rain storms with an associated hydrograph rise above the level of background noise were determined to have had a stormflow response. For these rain storms, we next identified the start and end times of the stormflow hydrograph response. The methods for identifying these times were adapted from the Rainfall Runoff Event Detection and Identification (RREDI) toolkit (Canham et al. 2025), an automated time-series event separation algorithm. A detailed description of each step of

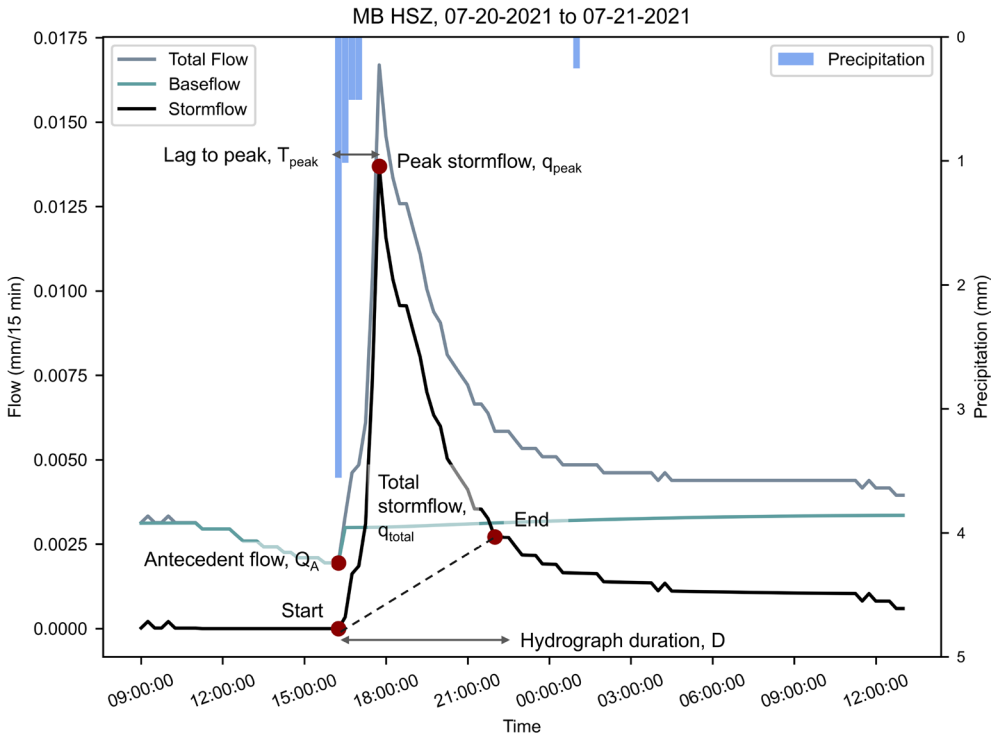

FIGURE 2 | Example of baseflow separation and a stormflow response showing total stormflow (q_{total}), lag to peak time (T_{peak}), hydrograph duration (D), peak stormflow (q_{peak}), and start and end times in the moderately burned high snow zone (HSZ).

TABLE 2 | Predictor and response variables considered for this study. The bold line separates continuous predictors (above) from categorical predictors (below).

Type	Variable	Name	Unit
Predictor	MI_{60}	Maximum rainfall intensity over 60 min	mm h^{-1}
	PWD	Cumulative potential water deficit from the day before an rain storm	mm
	year	Year	
	zone	Snow zone (high snow zone HSZ, low snow zone LSZ)	
	burn	Burn category (unburned UB, severely burned SB, moderately burned MB)	
Response	S	Stage rise	cm
	q_{peak}	Peak stormflow	mm
	q_{total}	Total stormflow	mm
	T_{peak}	Lag to peak time	hr

the algorithm is available in the paper's Supplement, along with justifications for each decision. Using a search window beginning four time steps before the rain storm start and ending at the time of the peak stormflow, the stormflow response start was assigned when the first derivative of the stormflow exceeded a threshold of 0.0001. We allowed for a hydrograph rise to start before the rain storm start time because the 1 km grid size of the MRMS data is close to the area of the catchments, and we wanted to allow for the possibility that rain began on a partial section of the catchment before it was reported by the MRMS grid cell. If no values exceeded the threshold for response, then the start time of the hydrograph response was set as the start of the rain storm. The hydrograph end was identified after the flow was reduced from its peak magnitude by 80%; the precise time was selected as either the next occurrence of a local minimum or when the first derivative of the flow stayed between 0 and a threshold of −0.005 for 5 h, whichever occurred first. If no end was identified by this process within 24 h of the event hydrograph peak, the calculation was repeated with a peak magnitude reduction of 60% instead of 80%. The thresholds were determined through trial and error as producing the most accurate start and end times. After storm hydrographs were automatically identified this way for all sites, the hydrographs were reviewed to delete those that contained missing data or were visually indistinguishable from background noise.

Once rain storms had been identified and quality controlled, the following stormflow response metrics were computed to characterise stormflow magnitude: total stormflow (q_{total}; mm) and magnitude of peak stormflow (q_{peak}; mm) (Figure 2). In addition to recording the change in flow for a rain storm, we also measured stage rise (S; cm) because several rating curves had high levels of uncertainty (Figure S1). To characterise stormflow timing, we computed lag to peak time (T_{peak}; h) using the time when 50% of the rain had fallen during each event. The lag to peak is the difference between the 50% rainfall time and the peak stormflow time (Table 2).

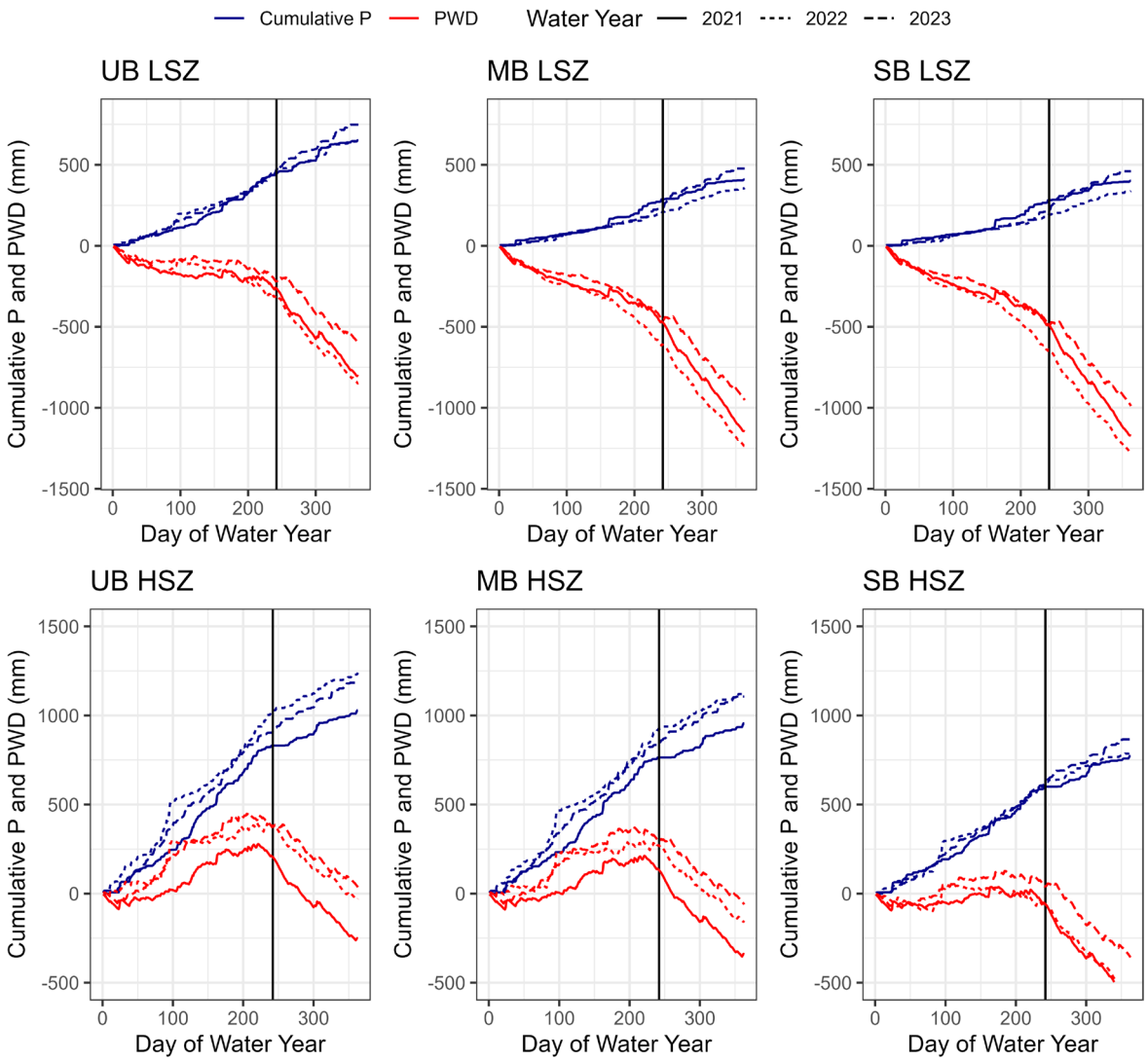

FIGURE 3 | Differences in cumulative precipitation (Cumulative P) and cumulative potential water deficit (PWD) for each catchment (HSZ- high snow zone; LSZ- low snow zone) over the study period. The vertical line is June 1.

2.4 | Factors Affecting Stormflow Responses

Our study objectives were to (1) evaluate whether the stormflow responses varied between burn categories and snow zones, and (2) examine the factors affecting stormflow response. These two objectives are inter-related in our analysis because the sample size of catchments is small: six total, with each representing a different combination of burn category and snow zone. We hypothesised that multiple factors would affect stormflow responses: rainfall variables, antecedent moisture, burn severity, snow zone, and year post-fire. To test this hypothesis, we developed generalised linear models (GLM) for each of the four target stormflow responses, where the individual stormflow metric (dependent variable) was modelled as a function of the combined effects of predictor variables: burn category (unburned, moderate burn, severe burn), snow zone (HSZ or LSZ), year post-fire (0, 1, 2, 3), a rainfall variable, and an antecedent moisture variable. The rainfall variables considered were depth, duration, and maximum intensities for rain storms. We examined correlations of each of these with stormflow response metrics and selected MI_{60} due to the highest correlation with stage rise. For antecedent wetness conditions, we considered antecedent flow (Q_A; mm), the baseflow at the rain storm start time (Hammond and Kampf 2020) (Figure 2). We also tested the cumulative potential water deficit value from the day before a rain storm (PWD) (Figure 3). PWD is the daily precipitation minus the daily reference evapotranspiration extracted for each catchment from gridMET (Abatzoglou 2011). This is an indication of whether a location is likely to have a water surplus or water deficit. Values of PWD can be accumulated over time to represent patterns of catchment wetting and drying. We calculated cumulative values of PWD starting on the first day of each water year. The cumulative PWD is the sum of the previous day's cumulative PWD plus the current day's PWD. Of the two antecedent wetness metrics, PWD was a stronger predictor of most stormflow responses. Given moderate collinearity among these variables, Q_A was omitted as a predictor. Table 2 describes the predictor variables selected for analysis.

Data distribution varied among the stormflow metrics; therefore, a gamma distribution was used to model the q_{total}, q_{peak}, and S

metrics, as they were all right-skewed and > 0. The T_{peak} metric was normally distributed and was modelled using a Gaussian distribution. Both gamma and Gaussian GLMs were evaluated for model fit using posterior predictive checks to assess the normality of residual distributions, homogeneity of variance, and for variable collinearity using the 'performance' package in *R* (Lüdecke et al. 2021). After model fitting and testing, we used three different methods for interpreting model output and addressing research hypotheses. First, we evaluated model performance and predictor importance using partial R^2 calculated from the 'rsq' package in *R* and transformed it to % total variance explained (model R^2/predictor partial R^2). This allows for the evaluation of the relative contribution of each predictor to total model explained variance (Zhang et al. 2016). Second, we calculated the estimated marginal means (EMM) for categorical predictors (snow zone, burn severity) using the 'emmeans' package in *R* (Lenth et al. 2020). Estimated marginal means differ from descriptive means (calculated from observations within a factor-level) in that they are estimated from the GLM (rather than from the data) using a reference grid that combines different values for each model predictor. In this manner, they represent the average response for each level of a factor while holding other predictors at a constant value. After EMMs were calculated, they were tested for significant pairwise differences using a Tukey adjustment for multiple comparisons. Comparisons were considered significantly different when $p < 0.05$. Finally, to visualise shape and size of the stormflow responses to continuous predictors (MI60, PWD, and year), we developed partial dependence plots using the 'pdp' package in *R* (Greenwell 2017).

Because of high uncertainty in the discharge metrics, we conducted an uncertainty analysis for the GLMs of q_{total} and q_{peak}. The methods and results for this analysis are presented in the Supplement.

3 | Results

3.1 | Differences Between Snow Zones and Burn Categories

Our first objective was to evaluate whether stormflow responses varied by snow zone and by burn category. Since multiple factors vary simultaneously between the catchments, we evaluated these differences as part of the generalised linear model results, using estimated marginal means (EMMs). Pairwise comparisons of EMM for the response variables (q_{total}, q_{peak}, T_{peak}, and S) show differences between snow zones and burn severity (Figure 5). Comparing the unburned catchments in each snow zone, estimated marginal means for q_{total}, q_{peak}, and T_{peak} were significantly higher in the HSZ ($p < 0.05$), with only S being more similar between zones (Figures 4B and 5). These results indicate that the HSZ produces higher event flow and peak flow than the LSZ. In contrast, the effects of burn category were not clear for most of the response variables. S had the biggest difference in EMM between unburned and severely burned in the LSZ, with substantially higher S in the severely burned catchment compared to the unburned. In the HSZ, T_{peak} in both moderate and severely burned catchments was significantly lower than unburned, indicating that the burned catchments responded more quickly to rainfall.

3.2 | Drivers of Stormflow Response

The GLM results indicate relative contributions of predictor variables to stormflow responses (Figure 6). For all the stormflow magnitude metrics (q_{total}, q_{peak}, S), MI_{60} was the largest contributor, with more variance explained by MI_{60} in the HSZ than in the LSZ. Burn category and year post-fire also explained some of the variance in flow metrics, but contributions of PWD were minimal. For T_{peak}, burn category was the largest contributor. Year post-fire and PWD contributed only to predictions of lag to peak in the LSZ.

Partial dependence plots show how stormflow varies in the model in response to continuous predictors; these plots demonstrate differences in the responses by snow zone and among burn severity categories within snow zones (Figure 7). Tighter clustering of responses between dashed versus solid lines indicates little effect of snow zone, whereas more space between solid and dashed lines indicates a snow zone effect. Within a snow zone line group (solid or dashed), tighter clustering indicates little burn severity impact, whereas more separation indicates a stronger effect of burn severity. The three stormflow magnitude metrics (q_{total}, q_{peak}, S) all increase with MI_{60}, with greater increases in the HSZ for q_{total} and q_{peak}. For PWD, the range of values is distinct between snow zones, with higher moisture (PWD) in the HSZ. In general, the stormflow variables did not change substantially with increasing PWD, except for q_{total} in the HSZ, which had an exponential increase. The effects of year were limited for all stormflow magnitude variables.

The stormflow timing (T_{peak}) decreased slightly with greater MI_{60} in the HSZ but increased slightly in the LSZ. These effects did not vary by snow zone or burn category, except the unburned HSZ site had a much longer T_{peak} than all other sites. In the LSZ, T_{peak} decreased with increasing PWD, whereas the opposite direction of response was evident in the HSZ. T_{peak} also increased with year post-fire in the LSZ but slightly decreased with year post-fire in the HSZ. Overall, the partial dependence plots illustrate the dominance of MI_{60} in influencing the stormflow magnitude responses and less influence of the predictor variables for stormflow timing.

4 | Discussion

4.1 | Differences in Stormflow Response by Snow Zone

We expected to find differences in stormflow responses by snow zone because of their very different hydrologic regimes. Along the Front Range, high elevation catchments with deep winter snow have been found to contribute more flow per unit area than those in areas of patchy snow cover (Hammond et al. 2018). Harrison et al. (2021) described an abrupt shift in hydrologic regime between the HSZ and the LSZ in the Cache la Poudre basin; discharge and runoff ratios were orders of magnitude higher at high elevation catchments compared to lower snow catchments. In contrast to this prior research, the differences we found in rainfall responses between HSZ and LSZ in this study were not as large. The HSZ produced higher total stormflow than the ISZ by about a factor of three, and

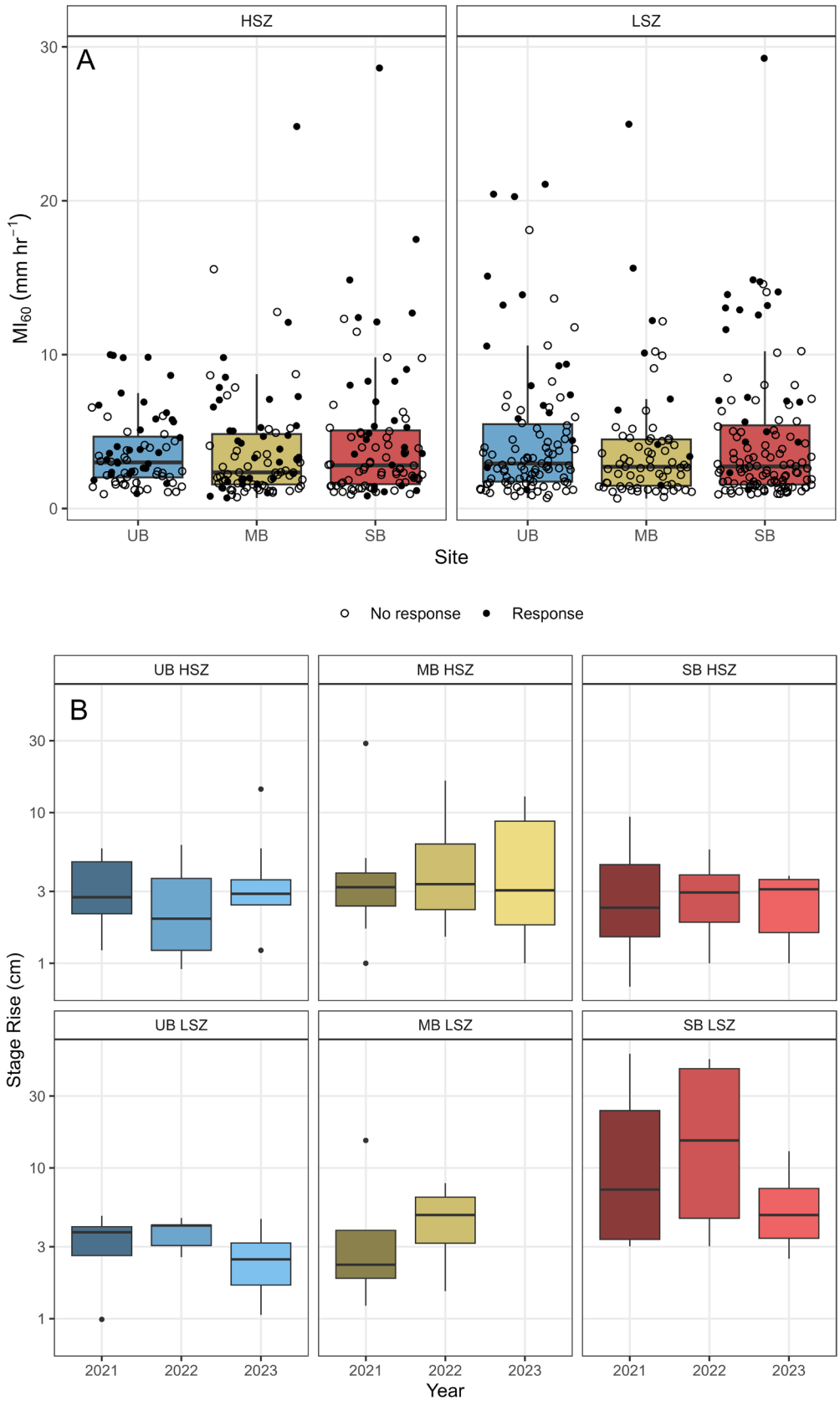

FIGURE 4 | Plots showing (A) the range of maximum rainfall intensity over 60 min (MI_{60}) by snow zone and catchment (HSZ—high snow zone; LSZ—low snow zone) and (B) stage rise (S) over time for each site, plotted on a log scale. Filled points in A indicate that a value of MI_{60} produced a quickflow response.

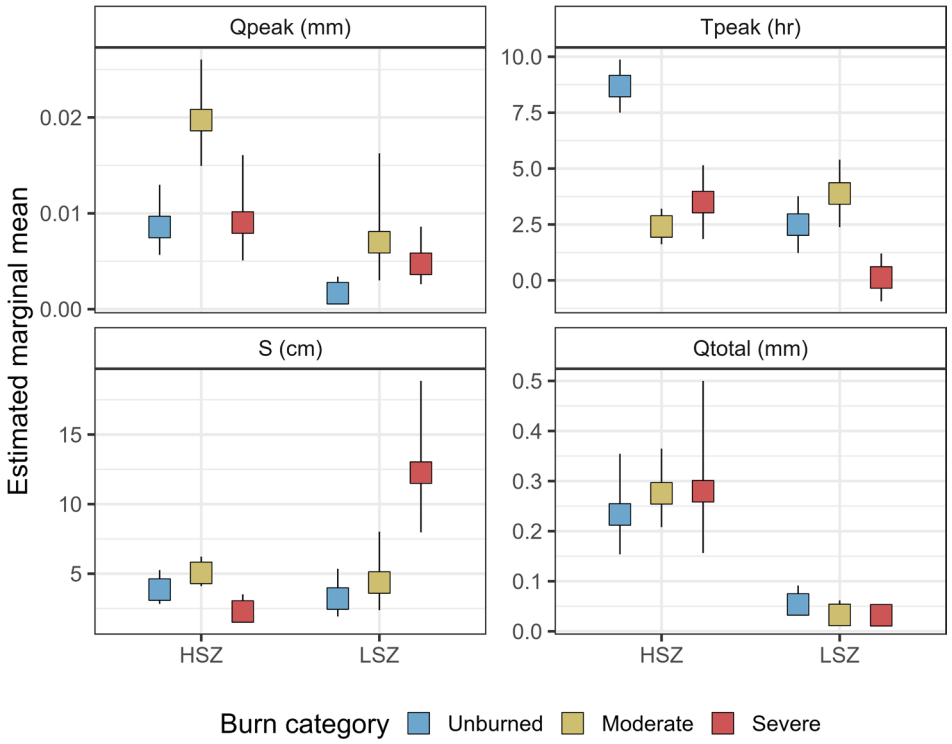

FIGURE 5 | Estimated marginal mean (EMM) of modelled stormflow response variables by burn category and snow zone (HSZ- high snow zone; LSZ- low snow zone) with asymmetric 95% confidence intervals.

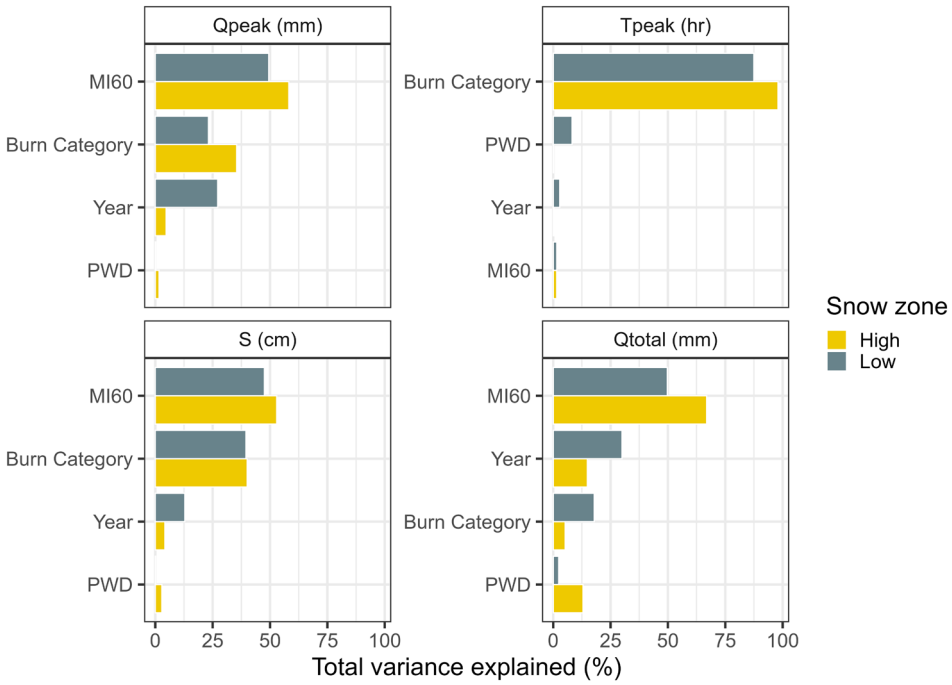

FIGURE 6 | Behaviour of the logistic generalised linear model for the four stormflow response models visualised by partial R^2 plots.

peak flows also tended to be higher for the HSZ compared to the LSZ (Figure 7). The elevated flow responses in the HSZ likely relate to higher soil moisture. Harrison et al. (2021) found that volumetric water content (VWC) in the persistent snow region of the Cache la Poudre basin ranged from 0.2 to 0.6 between 2016 and 2019, compared to 0.1 to 0.2 for transitional-intermittent (low snow) sites. Unfortunately, we did not have soil moisture data available for this study period, but the potential water deficit (PWD) does indicate more water in the HSZ than the ISZ (Figure 3). By the start of the rainy season each year, all LSZ catchments were already in water deficit (negative PWD), whereas HSZ catchments still had some water surplus. Despite the large differences in PWD between snow zones, the differences in PWD within snow zones

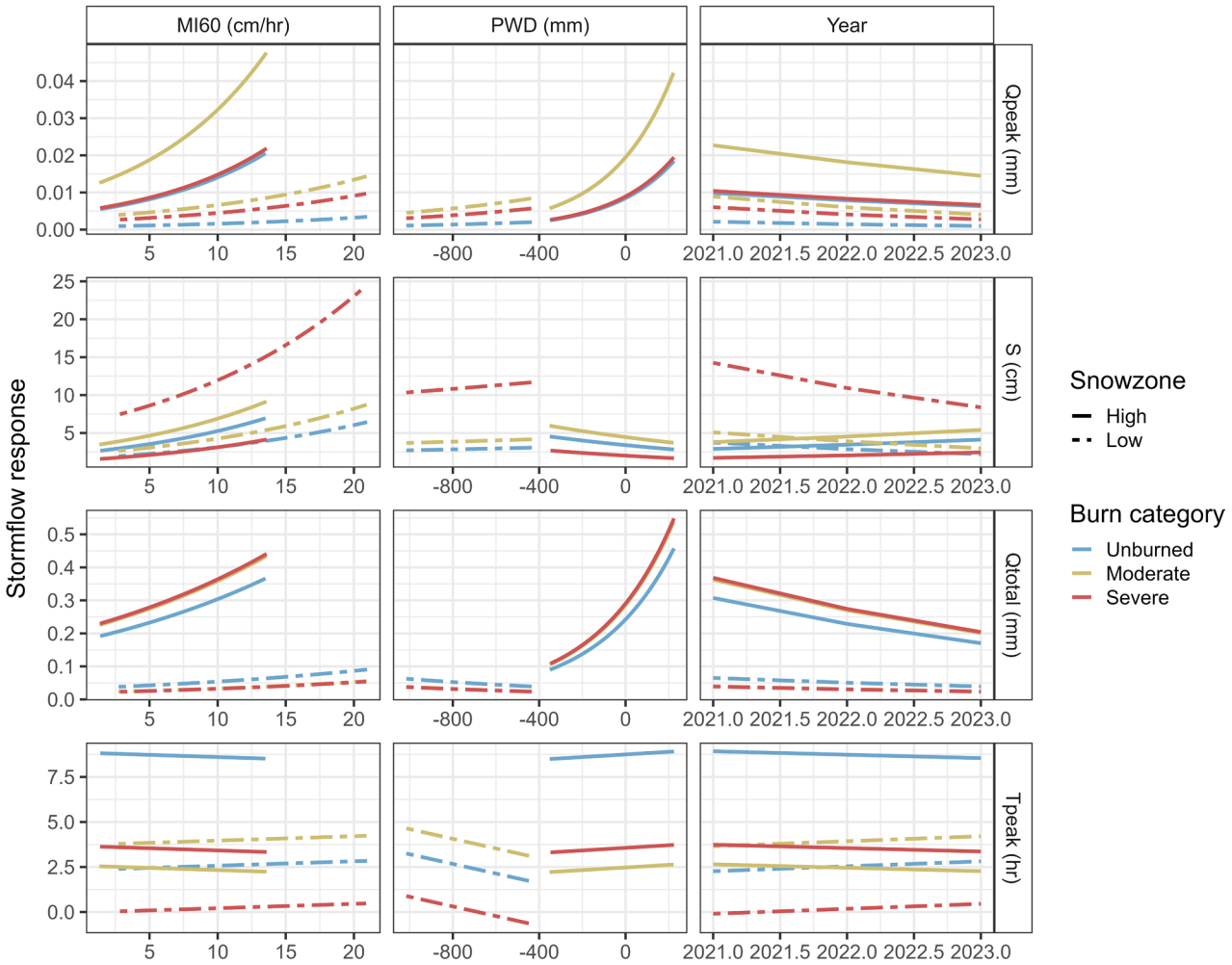

FIGURE 7 | Behaviour of the logistic generalised linear model for the four stormflow response models visualised by partial dependence plots and shown for burn category and snow zone.

were much more subtle, and this may be why PWD was not a strong predictor for most of the stormflow response metrics (Figure 6).

Other studies have found that antecedent wetness conditions are important drivers of stormflow response: wet antecedent conditions were shown to be correlated with significantly higher runoff in an unburned catchment in New Mexico (Schoener and Stone 2019). Penna et al. (2011) found that soil moisture exhibited a threshold relationship to runoff, with stormflow abruptly increasing when VWC exceeded 45%. They theorised that after this threshold is exceeded, the hillslope becomes 'hydrologically active' and delivers a significant amount of subsurface flow to the stream. Wetter hillslope conditions are also correlated with the expansion of macropore systems, allowing larger volumes of water to move through the subsurface in the same amount of time (Sidle et al. 1995). In our study, the soil moisture in the LSZ was likely very low throughout each summer rainy season, as indicated by negative PWDs (Figure 3), so antecedent conditions were not wet enough to produce the types of stormflow responses documented in other studies. Slightly more influence of PWD is evident in the HSZ, particularly where PWD becomes positive (Figure 3), indicating that antecedent conditions have a greater influence on stormflow when conditions are wetter.

4.2 | Differences in Stormflow Response by Burn Category

Effects of burn category on storm response were somewhat ambiguous. In the LSZ, the only clear burn effect on stormflow response was stage rise at the severely burned site, which was significantly higher than stage rises in the unburned and moderately burned sites (Figures 5 and 8). SB LSZ did have some large stormflow responses that overtopped the sensor housing, caused debris to pile up behind the sensor housing, and changed the channel geometry (Figure 9). The stage data at this site also showed numerous instances of bed aggradation and incision, more than the other catchments. The changes in channel geometry made the stage-discharge rating curve highly uncertain at this site. Had it been possible to quantify storm discharge reliably, the flow peak and total event flow at SB LSZ would likely have been higher than at the other LSZ sites. The highest storm responses at SB ISZ were likely caused by infiltration excess overland flow, based on field evidence of surface erosion and the low lag to peak at this site. For a catchment of this size, the lag to peak for infiltration excess overland flow would be on the order of 1 h (Dunne 1983), which is consistent with the lag times observed at SB ISZ (Figure 5). The longer lags to peak at the other LSZ

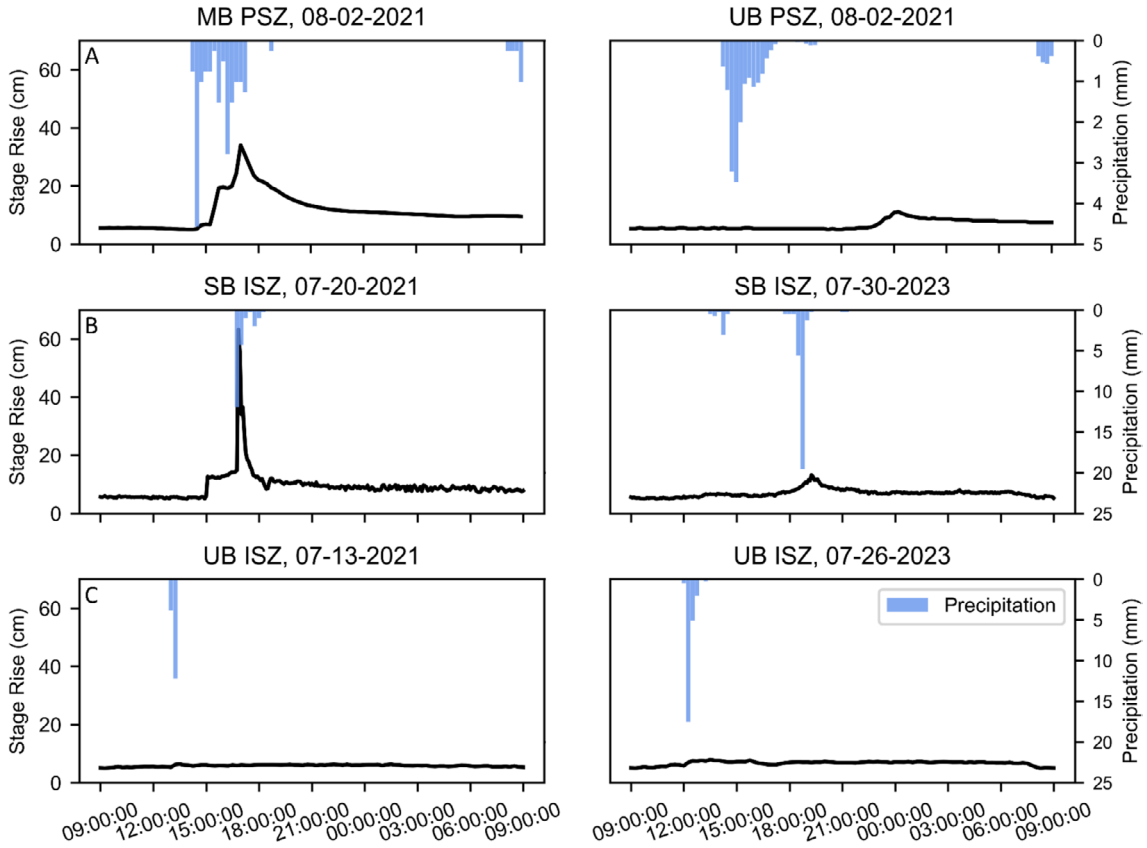

FIGURE 8 | Examples of the difference in stage rise (S) between (A) the moderately burned (MB) and unburned (UB) catchments in the high snow zone (HSZ) for the same rain event on August 2, 2021, (B) similarly sized rain events in severely burned (SB) low snow zone (LSZ) sites in 2021 and 2023, compared to (C) similarly sized rain events at unburned LSZ in 2021 and 2023. The data have been adjusted to start at 5 cm to better facilitate comparisons.

sites, on the order of 2–5 h, indicate subsurface pathways are more likely the source of stormflow. This is consistent with prior research on burn effects in the region, where infiltration excess overland flow is common after moderate-high severity burn but not as common for low severity or unburned sites (Robichaud and Waldrop 1994). However, in prior research, the effects of burn severity on runoff generation have been inconsistent (Vieira et al. 2015), and this may be why we did not detect significant differences by burn category in some stormflow metrics.

We saw very little evidence of infiltration excess overland flow in the HSZ, and the lag to peak times (Figure 5) also suggests that stormflow came mostly from subsurface flow. Burning may have increased the peak flow and decreased the lag to peak (Figure 8), but those potential burn effects could just as easily have been caused by other differences between catchments. For example, SB HSZ had the lowest snow persistence of the three catchments in that zone (Table 1), whereas the unburned catchment had the highest snow persistence. Because of the lower snow at SB HSZ, the antecedent moisture may have been lower, leading to lower stormflow responses compared to the other HSZ catchments. The SB HSZ site is also located on a steep channel, much steeper than we would normally choose for a stream gauging site. We chose this site because of the high burn coverage in the contributing area, but the steep slope may have contributed to some flow losses to the subsurface along the stream reach. We also learned after installing the site that the drainage area contains former glacial and landslide deposits, which likely makes it highly permeable, another reason why more water may have infiltrated deep into the subsurface, bypassing the stream gauge. In contrast, the MB HSZ monitoring site is in a more gently sloping section of channel that is less likely to be losing as much flow to the subsurface. This difference in channel properties may be enough to obscure any burn effects on stormflow magnitude.

Another challenge in discerning the burn effects in the study catchments is the differences in burn patterns between them. The spatial coverage of low, medium, and high severity is different for all the burned catchments (Figure 1; Table 1). All the MB and SB catchments had >20% of the area burned, and based on prior research, this should have been enough to produce a change in streamflow from unburned conditions (Goeking and Tarboton 2020; Williams et al. 2022). However, we did not have streamflow data prior to burning to determine how each individual catchment's stormflow changed from before to after wildfire. Our study approach, including unburned control sites compared to fire-impacted sites, is relatively unusual for post-fire hydrologic studies, and an expanded number of burned and unburned catchments would help us better distinguish which stormflow responses are likely a result of fire

FIGURE 9 | Geomorphic change observed at severely burned, low snow zone. After a large rainstorm on June 25, 2021, the stream sensor was covered with ~10 cm of fine sediment. The debris marking the upper levels of the staff plate implies that a large amount of sediment was moved downstream. Photograph courtesy of Stephanie Kampf.

and which are caused by other sources of variability between catchments.

4.3 | Recovery Over Time

Many studies have shown that post-fire hydrologic impacts are greatest in the first few years following a wildfire, and that recovery to pre-fire conditions is variable and depends on a variety of factors including vegetation regrowth, rainfall regime, channel hydraulic roughness, and the reduction of soil-water repellency (Ebel et al. 2022; Kinoshita and Hogue 2011; Kunze and Stednick 2006; Liu et al. 2021; Moody and Martin 2001; Wilson et al. 2018). In this study, year did contribute to modelled q_{peak}, q_{total}, and S (Figure 6), but the magnitude of the effect was small compared to that of MI_{60} (Figure 7). This indicates that the effects of vegetation recovery on post-fire stormflow response can be obscured by the variability in storm characteristics between years. All the burned sites experienced some vegetation regrowth over the study period, with higher vegetation recovery in the LSZ compared to the HSZ. However, vegetation regrowth is most effective at reducing stormflow responses where it shifts stormflow generation from infiltration excess overland flow to subsurface flow. Since all the sites except SB LSZ mostly experienced subsurface flow responses to rain, the vegetation regrowth did not cause a change in the stormflow generation pathways.

4.4 | Implications

There has been limited prior research on the post-fire hydrologic impact on rainfall-runoff in high elevation, high snow environments. With these areas experiencing larger and more frequent fires, it is critical to understand if these regions carry the same risks of flooding and debris flows seen at lower elevations (Alizadeh et al. 2021; Higuera et al. 2021). The results of this study suggest that the high snow zone does not experience the infiltration excess overland flow that creates high post-fire floods. The burned HSZ sites responded to many rain storms, even those with very low rainfall intensities, but the responses were generally small, with only a few centimetres of stage rise. Their high responsiveness to rain is most likely related to deeper and longer lasting snowpack leading to high antecedent soil moisture during the summer months.

Our findings indicate that all the study streams are most responsive to rainfall intensity compared to other predictors. In Colorado, precipitation intensities from summer storms are expected to increase due to climate change (Bolinger et al. 2024). Since the 1950s, the total contribution of heavy and extreme precipitation to annual precipitation has increased in Colorado and other areas of the Southwest (USGCRP 2017), and Kunkel et al. (2020) found that between 1949–2016 and 1979–2016, precipitation amounts from heavy (1-, 2-, 5-, and 10-year) and borderline extreme (20-year) storms generally rose across various regions in this area as well. Climate models project overall increases in the magnitudes of heavy and extreme rainfalls (Swain et al. 2020; Rupp et al. 2022; Pierce et al. 2023). These increases were more pronounced and consistent during the warm season compared to the cold season. In contrast, winter precipitation in the West has steadily decreased in the past few decades, with losses of up to 60% predicted within the next century (Fyfe et al. 2017; Rhoades et al. 2018; Wi et al. 2012). Though high elevation areas are likely to remain places of deep winter snow accumulation, a shorter winter season with earlier melt times could lead to drier summer soils in the HSZ (Gergel et al. 2017; Hammond et al. 2023). Under these conditions, post-fire stormflow in high elevation areas could potentially be more severe than what we observed.

4.5 | Limitations

The goal of this analysis was to identify differences in the post-fire flow response between catchments of varying burn severity, across distinct elevation regions, and over time. There are several important limitations to consider when interpreting these results. First, the small sample size and short period of record introduce uncertainty as to whether the trends we identified hold true more generally. Second, post-fire stormflow generation is influenced by catchment attributes that can be highly variable and/or difficult to measure. Soil water repellency (Larsen et al. 2009; Woods et al. 2007), soil type (Miller et al. 2011), spatial patterns of burn severity (Cawson et al. 2013; Moody et al. 2008), and vegetation regrowth (Saxe et al. 2018; Bolotin and McMillan 2024) have all been identified in previous studies as influential in post-fire stormflow response, but it is difficult to separate out the effects of any one of these features on the overall catchment response. Third, data sources added

additional uncertainty to this analysis. Across the study catchments, a point-to-grid comparison between MRMS and tipping bucket data revealed a percent bias of −7% for MI_{60}, indicating that MRMS tends to slightly underestimate rainfall intensity compared to the tipping buckets. Stage data recorded by stream pressure transducers had a noise range of ~1 cm, making it difficult to accurately represent low flows and the start and end times of stormflow response intervals. The noise could have been lessened by using a moving average or median filter, or summing the data hourly or daily; however, we chose to leave the data as is to reflect the timing and magnitude of short duration stormflow responses more accurately. Two burned sites experienced geomorphic channel change along the study reach, leading to uncertainty in stream stage. Rating curves introduced further uncertainty in discharge, especially in cases of channel change where multiple rating curves were developed.

5 | Conclusions

This research examined how streams at different elevations and of differing burn severity responded to summer rain storms in years 1–3 following the Cameron Peak wildfire. Like previous studies, we found that catchments in the high snow zone produced more total stormflow than those in the mid-elevation low snow zone. Higher soil moisture content could explain why runoff was more likely in the HSZ; shallow groundwater near the streams could have enabled streams to respond to small rainfall inputs. The effects of burning on stormflow were evident in stage rise in the LSZ, whereas burning did not have a clear effect on stormflow in the HSZ. In the LSZ, the severely burned site experienced infiltration excess overland flow, as demonstrated by higher stage rises and shorter lags to peak than at other catchments. The effects of burning on stormflow in the HSZ were potentially obscured by other site differences in antecedent moisture, infiltration capacity, and channel morphology. Our findings highlight how the effects of burning on stormflow vary between catchments and across snow zones. When comparing stormflow responses among catchments, it can be difficult to separate the effects of fire from those of other catchment characteristics. Future studies that examine the post-fire hydrology of a larger number of high-elevation watersheds could help conclude whether these trends are representative across the Front Range and the western United States.

Acknowledgements

This study was funded by NSF EAR 2101068 and EAR 2302594. We thank Brian Ebel and two anonymous reviewers for their helpful comments and critique on earlier versions of this article. Any use of trade, firm, or product names is for descriptive purposes only and does not imply endorsement by the U.S. Government. We thank Rob Erskine and Tim Green for assistance with data collection and site maintenance.

Conflicts of Interest

The authors declare no conflicts of interest.

Data Availability Statement

The data that support the findings of this study are openly available from HydroShare (Miller et al. 2025).

References

Abatzoglou, J. T. 2011. "Development of Gridded Surface Meteorological Data for Ecological Applications and Modelling." *International Journal of Climatology* 33, no. 1: 121–131. https://doi.org/10.1002/joc.3413.

Addington, R. N., G. H. Aplet, M. A. Battaglia, et al. 2018. Principles and practices for the restoration of ponderosa pine and dry mixed-conifer forests of the Colorado Front Range.

Alizadeh, M. R., J. T. Abatzoglou, C. H. Luce, J. F. Adamowski, A. Farid, and M. Sadegh. 2021. "Warming Enabled Upslope Advance in Western US Forest Fires." *Proceedings of the National Academy of Sciences* 118, no. 22: e2009717118. https://doi.org/10.1073/pnas.2009717118.

BAER. 2020. Cameron Peak Fire Forest Service Burned Area Emergency Response Executive Summary Arapaho Roosevelt National Forest December 15, 2020. US Forest Service.

Barnard, D. M., T. R. Green, K. R. Mankin, et al. 2023. "Wildfire and Climate Change Amplify Knowledge Gaps Linking Mountain Source-Water Systems and Agricultural Water Supply in the Western United States." *Agricultural Water Management* 286: 108377. https://doi.org/10.1016/j.agwat.2023.108377.

Bayabil, H. K., A. Fares, H. O. Sharif, D. T. Ghebreyesus, and H. A. Moreno. 2019. "Effects of Spatial and Temporal Data Aggregation on the Performance of the Multi-Radar Multi-Sensor System." *JAWRA Journal of the American Water Resources Association* 55, no. 6: 1492–1504. https://doi.org/10.1111/1752-1688.12799.

Bolinger, R. A., J. J. Lukas, R. S. Schumacher, and P. E. Goble. 2024. *Climate Change in Colorado*. 3rd ed. Colorado State University. https://doi.org/10.25675/10217/237323.

Bolotin, L. A., and H. McMillan. 2024. "A Hydrologic Signature Approach to Analysing Wildfire Impacts on Overland Flow." *Hydrological Processes* 38: e15215. https://doi.org/10.1002/hyp.15215.

Brown, T. C., M. T. Hobbins, and J. A. Ramirez. 2008. "Spatial Distribution of Water Supply in the Coterminous United States 1." *JAWRA Journal of the American Water Resources Association* 44, no. 6: 1474–1487. https://doi.org/10.1111/j.1752-1688.2008.00252.x.

Calder, W. J., D. Parker, C. J. Stopka, G. Jiménez-Moreno, and B. N. Shuman. 2015. "Medieval Warming Initiated Exceptionally Large Wildfire Outbreaks in the Rocky Mountains." *Proceedings of the National Academy of Sciences* 112, no. 43: 13261–13266. https://doi.org/10.1073/pnas.1500796112.

Canham, H. A., B. Lane, C. B. Phillips, and B. P. Murphy. 2025. "Leveraging a Time-Series Event Separation Method to Disentangle Time-Varying Hydrologic Controls on Streamflow – Application to Wildfire-Affected Catchments." *Hydrology and Earth System Sciences* 29: 27–43. https://doi.org/10.5194/hess-29-27-2025.

Cawson, J. G., G. J. Sheridan, H. G. Smith, and P. N. J. Lane. 2013. "Effects of Fire Severity and Burn Patchiness on Hillslope-Scale Surface Runoff, Erosion and Hydrologic Connectivity in a Prescribed Burn." *Forest Ecology and Management* 310: 219–233. https://doi.org/10.1016/j.foreco.2013.08.016.

de Cicco, L. A., R. M. Hirsch, D. Lorenz, W. D. Watkins, and M. Johnson. 2024. dataRetrieval:R packages for discovering and retrieving water data available from Federal hydrologic web services, v.2.7.15. https://doi.org/10.5066/P9X4L3GE.

de Dios Benavis-Solorio, J., and L. H. MacDonald. 2005. "Measurement and Prediction of Post-Fire Erosion at the Hillslope Scale, Colorado Front Range." *International Journal of Wildland Fire* 14, no. 4: 457–474. https://doi.org/10.1071/WF05042.

Dunne, T. 1983. "Relation of Field Studies and Modeling in the Prediction of Storm Runoff." *Journal of Hydrology* 65, no. 1–3: 25–48.

Ebel, B. A., and J. A. Moody. 2013. "Rethinking Infiltration in Wildfire-Affected Soils." *Hydrological Processes* 27, no. 10: 1510–1514. https://doi.org/10.1002/hyp.9696.

Ebel, B. A., J. A. Moody, and D. A. Martin. 2012. "Hydrologic Conditions Controlling Runoff Generation Immediately After Wildfire." *Water Resources Research* 48: R011470. https://doi.org/10.1029/2011WR011470.

Ebel, B. A., J. W. Wagenbrenner, A. M. Kinoshita, and K. D. Bladon. 2022. "Hydrologic Recovery After Wildfire: A Framework of Approaches, Metrics, Criteria, Trajectories, and Timescales." *Journal Of Hydrology And Hydromechanics* 70, no. 4: 388–400. https://doi.org/10.2478/johh-2022-0033.

Fornwalt, P. J., L. S. Huckaby, S. K. Alton, M. R. Kaufmann, P. M. Brown, and A. S. Cheng. 2016. "Did the 2002 Hayman Fire, Colorado, USA, Burn With Uncharacteristic Severity?" *Fire Ecology* 12: 117–132. https://doi.org/10.4996/fireecology.1203117.

Fyfe, J. C., C. Derksen, L. Mudryk, et al. 2017. "Large Near-Term Projected Snowpack Loss Over the Western United States." *Nature Communications* 8, no. 1: 14996. https://doi.org/10.1038/ncomms14996.

Gergel, D. R., B. Nijssen, J. T. Abatzoglou, D. P. Lettenmaier, and M. R. Stumbaugh. 2017. "Effects of Climate Change on Snowpack and Fire Potential in the Western USA." *Climatic Change* 141: 287–299. https://doi.org/10.1007/s10584-017-1899-y.

Goeking, S. A., and D. G. Tarboton. 2020. "Forests and Water Yield: A Synthesis of Disturbance Effects on Streamflow and Snowpack in Western Coniferous Forests." *Journal of Forestry* 118, no. 2: 172–192. https://doi.org/10.1093/jofore/fvz069.

Greenwell, B. M. 2017. "Pdp: An R Package for Constructing Partial Dependence Plots." *R Journal* 9, no. 1: 421.

Hallema, D. W., F. N. Robinne, and K. D. Bladon. 2018. "Reframing the Challenge of Global Wildfire Threats to Water Supplies." *Earth's Future* 6, no. 6: 772–776. https://doi.org/10.1029/2018EF000867.

Hallema, D. W., G. Sun, K. D. Bladon, et al. 2017. "Regional Patterns of Postwildfire Streamflow Response in the Western United States: The Importance of Scale-Specific Connectivity." *Hydrological Processes* 31, no. 14: 2582–2598. https://doi.org/10.1002/hyp.11208.

Hammond, J. C. 2020. *Contiguous US annual snow persistence and trends from 2001-2020*. US Geological Survey data release. https://doi.org/10.5066/P9U7U5FP.

Hammond, J. C., and S. K. Kampf. 2020. "Subannual Streamflow Responses to Rainfall and Snowmelt Inputs in Snow-Dominated Watersheds of the Western United States." *Water Resources Research* 56: e2019WR026132. https://doi.org/10.1029/2019WR026132.

Hammond, J. C., F. A. Saavedra, and S. K. Kampf. 2018. "How Does Snow Persistence Relate to Annual Streamflow in Mountain Watersheds of the Western U.S. With Wet Maritime and Dry Continental Climates?" *Water Resources Research* 54: 2605–2623. https://doi.org/10.1002/2017WR021899.

Hammond, J. C., G. A. Sexstone, A. L. Putman, et al. 2023. "High Resolution SnowModel Simulations Reveal Future Elevation-Dependent Snow Loss and Earlier, Flashier Surface Water Input for the Upper Colorado River Basin." *Earth's Future* 11, no. 2: e2022EF003092. https://doi.org/10.1029/2022EF003092.

Harrison, H. N., J. C. Hammond, S. Kampf, and L. Kiewiet. 2021. "On the Hydrological Difference Between Catchments Above and Below the Intermittent-Persistent Snow Transition." *Hydrological Processes* 35, no. 11: e14411. https://doi.org/10.1002/hyp.14411.

Higuera, P. E., B. N. Shuman, and K. D. Wolf. 2021. "Rocky Mountain Subalpine Forests Now Burning More Than any Time in Recent Millennia." *Proceedings of the National Academy of Sciences* 118, no. 25: e2103135118. https://doi.org/10.1073/pnas.210313511.

Kampf, S. K., and M. A. Lefsky. 2016. "Transition of Dominant Peak Flow Source From Snowmelt to Rainfall Along the Colorado Front Range: Historical Patterns, Trends, and Lessons From the 2013 Colorado Front Range Floods." *Water Resources Research* 52, no. 1: 407–422. https://doi.org/10.1002/2015WR017784.

Kampf, S. K., D. McGrath, M. G. Sears, S. R. Fassnacht, L. Kiewiet, and J. C. Hammond. 2022. "Increasing Wildfire Impacts on Snowpack in the Western US." *Proceedings of the National Academy of Sciences* 119, no. 39: e2200333119. https://doi.org/10.1073/pnas.2200333119.

Kinoshita, A. M., and T. S. Hogue. 2011. "Spatial and Temporal Controls on Post-Fire Hydrologic Recovery in Southern California Watersheds." *Catena* 87, no. 2: 240–252. https://doi.org/10.1016/j.catena.2011.06.005.

Kunkel, K. E., T. R. Karl, M. F. Squires, X. Yin, S. T. Stegall, and D. R. Easterling. 2020. "Precipitation Extremes: Trends and Relationships With Average Precipitation and Precipitable Water in the Contiguous United States." *Journal of Applied Meteorology and Climatology* 59, no. 1: 125–142. https://doi.org/10.1175/JAMC-D-19-0185.1.

Kunze, M. D., and J. D. Stednick. 2006. "Streamflow and Suspended Sediment Yield Following the 2000 Bobcat Fire, Colorado." *Hydrological Processes: An International Journal* 20, no. 8: 1661–1681. https://doi.org/10.1002/hyp.5954.

Larsen, I. J., L. H. MacDonald, E. Brown, et al. 2009. "Causes of Post-Fire Runoff and Erosion: Water Repellency, Cover, or Soil Sealing?" *Soil Science Society of America Journal* 73, no. 4: 1393–1407. https://doi.org/10.2136/sssaj2007.0432.

Lenth, R. V., P. Buerkner, M. Herve, J. Love, H. Riebl, and H. Singmann. 2020. emmeans: estimated marginal means, aka least-squares means. 2020. R package version, 1(8).

Liu, T., L. A. McGuire, H. Wei, et al. 2021. "The Timing and Magnitude of Changes to Hortonian Overland Flow at the Watershed Scale During the Post-Fire Recovery Process." *Hydrological Processes* 35, no. 5: e14208. https://doi.org/10.1002/hyp.14208.

Lüdecke, D., M. S. Ben-Shachar, I. Patil, P. Waggoner, and D. Makowski. 2021. "Performance: An R Package for Assessment, Comparison and Testing of Statistical Models." *Journal of Open Source Software* 6, no. 60: 3139. https://doi.org/10.21105/joss.03139.

Lyne, V., and M. Hollick. 1979. "Stochastic Time-Variable Rainfall-Runoff Modelling." In *Institute of Engineers Australia National Conference*, 89–93. Institute of Engineers Australia.

Miller, M. E., L. H. MacDonald, P. R. Robichaud, and W. J. Elliot. 2011. "Predicting Post-Fire Hillslope Erosion in Forest Lands of the Western United States." *International Journal of Wildland Fire* 20: 982–999.

Miller, Q., M. Sears, D. Barnard, and S. Kampf. 2025. Cameron peak fire rainfall runoff data, HydroShare. http://www.hydroshare.org/resource/5ece16124a364db09a6ea9a7835ed257.

Moazami, S., and M. Najafi. 2021. "A Comprehensive Evaluation of GPM-IMERG V06 and MRMS With Hourly Ground-Based Precipitation Observations Across Canada." *Journal of Hydrology* 594: 125929. https://doi.org/10.1016/j.jhydrol.2020.125929.

Moody, J. A., and D. A. Martin. 2001. "Initial Hydrologic and Geomorphic Response Following a Wildfire in the Colorado Front Range." *Earth Surface Processes and Landforms: The Journal of the British Geomorphological Research Group* 26, no. 10: 1049–1070. https://doi.org/10.1002/esp.253.

Moody, J. A., D. A. Martin, S. L. Haire, and D. A. Kinner. 2008. "Linking Runoff Response to Burn Severity After a Wildfire." *Hydrological Processes: An International Journal* 22, no. 13: 2063–2074. https://doi.org/10.1002/hyp.6806.

Moody, J. A., R. A. Shakesby, P. R. Robichaud, S. H. Cannon, and D. A. Martin. 2013. "Current Research Issues Related to Post-Wildfire Runoff and Erosion Processes." *Earth-Science Reviews* 122: 10–37. https://doi.org/10.1016/j.earscirev.2013.03.004.

Moore, C., S. Kampf, B. Stone, and E. Richer. 2015. "A GIS-Based Method for Defining Snow Zones: Application to the Western United States." *Geocarto International* 30, no. 1: 62–81. https://doi.org/10.1080/10106049.2014.885089.

MTBS Data Access. 2017. Fire Level Geospatial Data MTBS Project (USDA Forest Service/U.S. Geological Survey). http://mtbs.gov/direct-download.

Nathan, R. J., and T. A. McMahon. 1990. "Evaluation of Automated Techniques for Base Flow and Recession Analyses." *Water Resources Research* 26, no. 7: 1465–1473. https://doi.org/10.1029/WR026i007p01465.

Penna, D., H. J. Tromp-van Meerveld, A. Gobbi, M. Borga, and G. Dalla Fontana. 2011. "The Influence of Soil Moisture on Threshold Runoff Generation Processes in an Alpine Headwater Catchment." *Hydrology and Earth System Sciences* 15: 689–702. https://doi.org/10.5194/hess-15-689-2011.

Pierce, D. W., D. R. Cayan, D. R. Feldman, and M. D. Risser. 2023. "Future Increases in North American Extreme Precipitation in CMIP6 Downscaled With LOCA." *Journal of Hydrometeorology* 24, no. 5: 951–975. https://doi.org/10.1175/JHM-D-22-0194.1.

R Core Team. 2024. R: A language and environment for statistical computing. R Foundation for Statistical Computing, Vienna, Austria. https://www.R-project.org/.

Rhoades, A. M., P. A. Ullrich, and C. M. Zarzycki. 2018. "Projecting 21st Century Snowpack Trends in Western USA Mountains Using Variable-Resolution CESM." *Climate Dynamics* 50: 261–288. https://doi.org/10.1007/s00382-017-3606-0.

Richer, E. E., S. K. Kampf, S. R. Fassnacht, and C. C. Moore. 2013. "Spatiotemporal Index for Analyzing Controls on Snow Climatology: Application in the Colorado Front Range." *Physical Geography* 34, no. 2: 85–107. https://doi.org/10.1080/02723646.2013.787578.

Rivera-Giboyeaux, A. M., and S.Weinbeck. 2024. "Evaluation of WSR-88D Level III and MRMS Rainfall Estimates Against Rain Gauge Observations at the Savannah River Site." *Journal of Operational Meteorology* 12, no. 7: 93–106. https://doi.org/10.15191/nwajom.2024.12072024.

Robichaud, P. R., and T. A. Waldrop. 1994. "A Comparison of Surface Runoff and Sediment Yields From Low-and High-Severity Site Preparation Burns 1." *JAWRA Journal of the American Water Resources Association* 30, no. 1: 27–34. https://doi.org/10.1111/j.1752-1688.1994.tb03270.x.

Rocca, M. E., P. M. Brown, L. H. MacDonald, and C. M. Carrico. 2014. "Climate Change Impacts on Fire Regimes and Key Ecosystem Services in Rocky Mountain Forests." *Forest Ecology and Management* 327: 290–305. https://doi.org/10.1016/j.foreco.2014.04.005.

Rupp, D. E., L. R. Hawkins, S. Li, M. Koszuta, and N. Siler. 2022. "Spatial Patterns of Extreme Precipitation and Their Changes Under~2°C Global Warming: A Large-Ensemble Study of the Western USA." *Climate Dynamics* 59, no. 7: 2363–2379. https://doi.org/10.1007/s00382-022-06214-3.

Samsonov, T. 2023. _grwat: River Hydrograph Separation and Analysis_. R Package Version 0.0.4. https://CRAN.R-project.org/package=grwat.

Saxe, S., T. S. Hogue, and L. Hay. 2018. "Characterization and Evaluation of Controls on Post-Fire Streamflow Response Across Western US Watersheds." *Hydrology and Earth System Sciences* 22: 1221–1237. https://doi.org/10.5194/hess-22-1221-2018.

Schoener, G., and M. C. Stone. 2019. "Impact of Antecedent Soil Moisture on Runoff From a Semi-Arid Catchment." *Journal of Hydrology* 569: 627–636.

Sidle, R. C., Y. Tsuboyama, S. Noguchi, I. Hosoda, M. Fujieda, and T. Shimizu. 1995. "Seasonal Hydrologic Response at Various Spatial Scales in a Small Forested Catchment, Hitachi Ohta, Japan." *Journal of Hydrology* 168: 227–250. https://doi.org/10.1016/0022-1694(94)02639-s.

Smith, R. S., R. D. Moore, M. Weiler, and G. Jost. 2014. "Spatial Controls on Groundwater Response Dynamics in a Snowmelt-Dominated Montane Catchment." *Hydrology and Earth System Sciences* 18, no. 5: 1835–1856. https://doi.org/10.5194/hess-18-1835-2014.

Swain, D. L., O. E. Wing, P. D. Bates, J. M. Done, K. A. Johnson, and D. R. Cameron. 2020. "Increased Flood Exposure due to Climate Change and Population Growth in the United States." *Earth's Future* 8, no. 11: e2020EF001778. https://doi.org/10.1029/2020EF001778.

U.S. Geological Survey. 2024a. USGS water data for the Nation: U.S. Geological Survey National Water Information System database. https://doi.org/10.5066/F7P55KJN.

U.S. Geological Survey. 2024b. USGS 3D Elevation Program 1-meter LiDAR Digital Elevation Model. https://elevation.nationalmap.gov/arcgis/rest/services/3DEPElevation/ImageServer.

USGCRP, D. J. Wuebbles, D. W. Fahey, et al. 2017. *Climate Science Special Report: Fourth National Climate Assessment*. U.S. Global Change Research Program. https://doi.org/10.7930/J0J964J6.

Vieira, D. C. S., C. Fernández, J. A. Vega, and J. J. Keizer. 2015. "Does Soil Burn Severity Affect the Post-Fire Runoff and Interrill Erosion Response? A Review Based on Meta-Analysis of Field Rainfall Simulation Data." *Journal of Hydrology* 523: 452–464.

Viviroli, D., H. H. Dürr, B. Messerli, M. Meybeck, and R. Weingartner. 2007. "Mountains of the World, Water Towers for Humanity: Typology, Mapping, and Global Significance." *Water Resources Research* 43: W07447. https://doi.org/10.1029/2006WR005653.

Westerling, A. L. 2016. "Increasing Western US Forest Wildfire Activity: Sensitivity to Changes in the Timing of Spring." *Philosophical Transactions of the Royal Society, B: Biological Sciences* 371, no. 1696: 20150178. https://doi.org/10.1098/rstb.2015.0178.

Westerling, A. L., M. G. Turner, E. A. Smithwick, W. H. Romme, and M. G. Ryan. 2011. "Continued Warming Could Transform Greater Yellowstone Fire Regimes by Mid-21st Century." *Proceedings of the National Academy of Sciences* 108, no. 32: 13165–13170. https://doi.org/10.1073/pnas.1110199108.

Wi, S., F. Dominguez, M. Durcik, J. Valdes, H. F. Diaz, and C. L. Castro. 2012. "Climate Change Projection of Snowfall in the Colorado River Basin Using Dynamical Downscaling." *Water Resources Research* 48, no. 5: W05504. https://doi.org/10.1029/2011WR010674.

Williams, A. P., B. Livneh, K. A. McKinnon, et al. 2022. "Growing Impact of Wildfire on Western US Water Supply." *Proceedings of the National Academy of Sciences* 119, no. 10: e2114069119.

Wilson, C., S. K. Kampf, J. W. Wagenbrenner, and L. H. MacDonald. 2018. "Rainfall Thresholds for Post-Fire Runoff and Sediment Delivery From Plot to Watershed Scales." *Forest Ecology and Management* 430: 346–356. https://doi.org/10.1016/j.foreco.2018.08.025.

Woods, S. W., A. Birkas, and R. Ahl. 2007. "Spatial Variability of Soil Hydrophobicity After Wildfires in Montana and Colorado." *Geomorphology* 86: 465–479. https://doi.org/10.1016/j.geomorph.2006.09.015.

Zhang, J., K. Howard, C. Langston, et al. 2016. "Multi-Radar Multi-Sensor (MRMS) quantitative precipitation estimation: initial operating capabilities." *Bulletin of the American Meteorological Society* 97, no. 4: 621–638. https://doi.org/10.1175/bams-d-14-00174.

Supporting Information

Additional supporting information can be found online in the Supporting Information section.